https://doi.org/10.17221/125/2022-PPS

Comparison of gene expression changes in two wheat varieties with different phenotype to stripe rust using RNA-seq analysis

Congying Yuan, Yadi Miao, Huihan Zhang, Shiying Liu, Yaoyao Wang*

College of Life Sciences, Luoyang Normal University, Luoyang, PR China

**Corresponding author: pingboycy@163.com*

Citation: Yuan C.Y., Miao Y.D., Zhang H.H., Liu S.Y., Wang Y.Y. (2023): Comparison of gene expression changes in two wheat varieties with different phenotype to stripe rust using RNA-seq analysis. Plant Protect. Sci., 59: 134–144.

Abstract: The fungus *Puccinia striiformis* f. sp. *tritici* (Pst) is an important threat to wheat production because it can cause wheat stripe rust. The present study aimed to identify new stripe rust resistance genes and to provide a theoretical and practical basis for breeding wheat varieties with broad spectrum, stable, and durable resistance. Wheat leaves inoculated with wheat stripe rust fungus Chinese yellow rust 34 were collected at different time points for transcriptomic analysis based on the wheat stripe rust susceptible varieties AVOCET S (AVS) and AVSYr15NIL [near-isogenic line (NIL) derived from AVS]. The results showed that the number of upregulated genes in the two varieties was 294, 364, 398, and 604, and the number of downregulated genes was 520, 178, 570, and 345 on the 1st, 3rd, 5th, and 7th days post inoculation, respectively. Gene Ontology and Kyoto Encyclopedia of Gene and Genomes enrichment analyses found enrichment of differentially expressed genes in the peroxisome proliferators-activated receptor signaling pathways, plant–pathogen interaction, and styrene acrylic acid biosynthesis that encoded protein kinases, signal transduction, transcription factors, and functional protein components. Differentially expressed genes were randomly selected for quantitative reverse transcription PCR analysis, and the change trend was the same as in the transcriptome data. The results of this study suggest that genes in AVSYr15NIL related to the stripe rust response could be valuable for understanding the mechanisms involved in stripe rust resistance.

Keywords: wheat stripe rust; RNA-seq; differentially expressed genes; DEGs; resistance

Wheat (*Triticum aestivum* L) is the most widely planted crop in the world due to its high nutritional value and common use (Ebeed 2022). Rust fungal diseases, commonly known as "jaundice" in China, are divided into stripe rust, stem rust, and leaf rust. Wheat rust is an important plant disease characterised by rapid spreading, which damages large areas of the wheat crop globally. Wheat stripe rust, the most serious among rust types (Chen 2005), occurs in many countries and regions around the world, including northern Europe, the northwestern United States, China, South America, Africa, India, the Middle East, the Mediterranean, Australia, and New Zealand (Wellings 2011). The disease is airborne, and thus it is difficult to control and prevent. At present, the plant-

Supported by a grant from the National Natural Science Foundation of China (No. 32202258); the Natural Science Foundation of Henan province, China (No. 202300410287); and the National Project Cultivation Fund of Luoyang Normal University, China (Grant No: 2018-PYJJ-005).

https://doi.org/10.17221/125/2022-PPS

ing of resistant cultivars and the application of fungicides are the main means of controlling stripe rust (Chen 2014). However, the large-scale popularisation and use of wheat disease-resistant varieties have led to selective pressure on wheat stripe rust groups, causing the formation of new pathogenic varieties of wheat stripe rust and resulting in the loss of disease resistance in wheat varieties. According to production practice and research, under normal circumstances, wheat varieties have disease resistance against specific pathogens, and they lose resistance to the pathogenicity of stripe rust fungi after 3–5 years of planting before new resistant varieties have been popularised and planted (Wan & Chen 2012). In addition, chemical control is widely used; although it has an immediate effect and can effectively control large-scale diseases in a short period, it can have serious implications for human health and the environment (Chen 2013). Cultivating wheat varieties with broad-spectrum, stable, and long-lasting disease resistance is the most economical and effective way to control wheat stripe rust.

Understanding the interactions between plants and pathogens and monitoring gene expression during this interaction are important for revealing the pathogenic mechanism of pathogens and the resistance mechanism of hosts (Colgan et al. 2017). Due to the large and complex genome of wheat, its genetic analysis is difficult, and stripe rust of wheat involves the entire life cycle of the main parasitic fungus. The complete life cycle involves two different families and genera of plants and comprises an asexual stage and a sexual stage. In the asexual stage, summer spores are produced and repeatedly infect wheat crops, while the sexual stage occurs in the transfer to *Berberis*, *Mahonia*, and other alternative hosts of *Puccinia striiformis* f. sp. *tritici* (Pst) (Zhao et al. 2016). Therefore, the cloning and functional study of wheat rust resistance genes have proceeded relatively slowly.

RNA sequencing (RNA-Seq) technology can be used to comprehensively study the gene function and specific biological processes of species at the transcriptional level (Xu et al. 2011). Using this technology, the gene expression level of the research object under a stressful environment can be examined. Thus, the technology can be used to explore the mechanism of the regulatory network of genes related to an organism's response and tolerance to stress (Haider et al. 2017). RNA-seq technology was first applied to growth and development in wheat research, and initial studies confirmed that the grain protein content (GPC) gene is an early regulator that can not only induce senescence but also redirect nutrients from leaves to fruit in a complex regulatory network (Cantu et al. 2011). RNA-seq technology has been widely used in wheat to cope with stress (Ma et al. 2021; Zhang et al. 2021; Lee et al. 2022; Vranic et al. 2022). At present, many candidate genes induced by stripe rust have been cloned and preliminarily analysed using RNA-seq, including TaWRKY, TaBCAT1, TaNAC30, TaEIL1, and TaSGT1 (Duan et al. 2013; Wang et al. 2018; Corredor-Moreno et al. 2021; Wang et al. 2022; Zhao et al. 2022). These results have provided a foundation for further analysis of the interaction between stripe rust and wheat's resistance to rust at the molecular level.

Yr15 shows broad-spectrum action against Pst variants. It was originally identified from wild emmer wheat and transferred into hexaploid common wheat using a chromosome 1BS translocation line (Klymiuk et al. 2018). AVSYr15NIL is a near-isogenic line in the common wheat AVOCET S background (Qie et al. 2019). To better understand the resistance mechanism of this gene, AVS and the AVS-dependent stripe rust-resistant near-isogenic line AVSYr15NIL, which contains the resistance gene *Yr15*, were used as the experimental materials, and RNA-seq technology was employed to screen differentially expressed genes after inoculation of CYR34 in this experiment. Using these two wheat varieties with different susceptibilities, this study aimed to reveal the mechanism of stripe rust resistance in wheat and explore additional resistance genes. The results provide a theoretical and practical basis for breeding wheat varieties with broad spectrum, stable, and durable resistance.

MATERIAL AND METHODS

Material handling and collection. Urediniospore multiplication: The wheat stripe rust race CYR34 preserved in liquid nitrogen was activated at 50 °C for 2 min, then mixed with talc (1 : 20) and inoculated into seedlings of the wheat cultivar AVS. Inoculated plants were placed in a dew chamber for 24 h at 10 °C without light and then moved to a growth chamber with a diurnal temperature cycle, gradually changing from 4 °C at 2:00 am

https://doi.org/10.17221/125/2022-PPS

to 20 °C at 2:00 pm, and with a 16 h light and 8 h dark cycle. After 17–20 days, the fresh urediniospores were collected.

Wheat cultivation and sample collection: The seeds of the wheat susceptible cultivar AVS (A) and the resistance cultivar AVSYr15NIL (Y) were sown in 7 cm × 7 cm × 7 cm plastic pots. When the seedlings reached the two-leaf one-minded stage, the fresh urediniospores of CYR34 were used to inoculate the seedlings. The inoculated plants were incubated in a dew chamber for 24 h and then in a growth chamber with the same conditions mentioned above. Samples were taken on the 1st, 3rd, 5th, and 7th days after inoculation and were named Y1, Y3, Y5, Y7, A1, A3, A5, and A7, respectively. The plants were preserved in liquid nitrogen for subsequent experiments. Each experiment was repeated three times.

RNA extraction, cDNA library construction, and sequencing. Total RNA was extracted from the wheat leaves with TriZol (Invitrogen, USA) following the manufacturer's instructions. The rRNA removal method was used to treat the total RNA. A DNA probe was hybridised to the rRNA, and then RNaseH was used to digest the DNA/RNA hybrid chain selectively. The DNA probe was digested with DNaseI, and the required RNA was obtained after purification. RNA was qualified using a NanoDrop 2000 UV-Vis spectrophotometer (NanoDrop, USA). RNA integrity was tested using an Agilent 2100 bioanalyser (Agilent Technologies, USA). Three replicates for each time point were performed for the RNA-seq.

The cDNA library construction used the chain-specific library building method. The first strand of cDNA was synthesised in an M-MuLV reverse transcriptase system using fragmented mRNA as a template and random oligonucleotides as primers, and then the first RNA strand was degraded by RNaseH while the second strand was synthesised by dNTPs in a DNA polymerase I system. The purified double-stranded cDNA was repaired at the end; a tail was added, and a sequencing adaptor was connected. AMPure XP beads were then used to screen 250–300 bp cDNA for PCR amplification, and AMPure XP beads were used to purify the PCR products and finally obtain the cDNA library. After construction, the library was initially quantified using a Qubit2.0 Fluorometer (Thermo Fisher Scientific, USA), diluted to 1.5 ng/uL, and then the insert size of the library was detected using an Agilent 2100 bioanalyser. qRT-PCR was used to accurately quantify the effective concentration of the library (library effective concentration higher than 2 nM) to ensure the quality of the library. After passing inspection, different libraries were pooled according to the requirements of effective concentration and targeting the off-machine data volume for Illumina sequencing.

The reads with low quality, contaminated joints, and high N content of unknown bases were deleted from the raw data to obtain clean data (clean reads). During the sequencing process, each cycle was monitored in real time, and the quality score of the original reading was higher than the ratio of the Q30 high-quality reading. Quality control was performed by calculating the guanine-cytosine (GC) content.

Differential expression analysis and differentially expressed genes. The software Bowtie2 (version 2.2.5) was used to align clean reads to the reference gene sequence. Then, RSEM (version 1.26.2) was used to calculate the gene expression level of each sample expressed as fragments per kilobase per million mapped to estimate gene expression levels. Clean reads were aligned to the reference genome (www.ncbi.nlm.nih.gov/dbEST/dbEST_summary.html) using HISAT (version 2.1.0). DESeq was used to perform differential expression analysis of duplicate biological samples. To designate changes in gene expression, a false discovery rate of 0.001 and log2 fold change were set as the threshold criteria for differential expression.

Functional annotation. Getorf (version EMBOSS:6.5.7.0) was used to detect the open reading frames (ORFs) of unigenes, and Hmmsearch (version 3.0) was used to align the ORFs to the transcription factor protein domains, and then annotate unigenes according to the characteristics of the transcription factor family described by Plant TFDB (http://planttfdb.gao-lab.org/). GO enrichment of differentially expressed genes was realised to determine gene functions. The Cluster of Orthologous Groups of proteins (COG) database was used to classify orthologous genes. KOBAS software (version 2.0) was used to analyse the enrichment of DEGs in KEGG (InterPro scan and the Kyoto Encyclopedia of Genes and Genomes) pathways to understand the functions and utilities of DEGs. Blast searches against the COG, GO, KEGG pathway, Swiss-Prot, and Non-redundant protein databases were employed to analyse the functions of DEGs.

https://doi.org/10.17221/125/2022-PPS

Gene expression level validation by qRT-PCR. Total RNA was used for library construction to synthesise cDNA. The first strand cDNA synthesis was performed using the Maxima® First cDNA Synthesis Kit (Fermentas, USA). A SYBR® Green I kit (TOYOBO, Japan) was used to perform quantitative PCR (qRT-PCR) in a CFX96 real-time PCR detection system (Bio-Rad, USA). The primers were designed based on randomly selected differentially expressed gene sequences. The procedure of the PCR reactions comprised a denaturing step for 10 min at 95 °C followed by 50 cycles of 15 s at 95 °C and a primer extension reaction at 55 °C for 1 minute. The TaRP15 gene was used as an internal control. All qRT-PCR tests were run in duplicate, each with three biological replicates. The primer information is listed in Table S1 in electronic supplementary material (ESM; for the ESM see the electronic version). The data were analysed using CFX96 software.

RESULTS

Transcriptome assembly analysis. Based on Sequencing by Synthesis (SBS) technology, the Illumina high-throughput sequencing platform was employed to construct mRNA-seq libraries to obtain clean reads, and a total of 302.474 Gb of clean data was obtained. The average amount of clean data for each sample was 9.42 Gb from the control and treatment libraries. The Q30 base percentage was above 92.19%, and the GC content was between 53.17% and 55.82%, indicating high sequencing accuracy (Table 1, Table S2 in ESM). The raw data of transcriptome sequencing have been submitted to NCBI under accession number PRJNA909039. The reference genomic source was http://www.wheatgenome.org/project/IWGSC-Bread-wheat-projects/reference-genome. The sequence comparison of the post-quality control sequencing data of each sample with the specified reference genome ranged from 89.036% to 93.291%, of which the unique alignment ratio was between 76.578% and 84.404%, and the contrast ratio was high. These results indicated that the data of transcriptome assembly were qualified for downstream analysis. The above data were analysed for expression; the analysis involved a total of 106 914 genes, of which 106 914 were known (78 755 expression levels). There were 132 624 transcripts, of which 132 624 (98 463 expression levels) were known.

Differentially expressed genes. Screening for differentially expressed genes (DEGs) was performed according to the gene difference multiple (fold change), and log2 fold change ≥ 1, *P*-value ≤ 0.05 were the criteria for being defined as an upregulated gene, while log2 fold change < –1 was defined as a downregulated gene. Figure 1A shows that after inoculating CYR34 for different days, the numbers of upregulated genes of the two varieties were 294, 364, 398, and 604, and the numbers of downregulated genes were 520, 178, 570, and 345.

After inoculation with CYR34, the specific numbers of DEGs in different inoculation periods were 498, 479, 477, and 238 (Figure 1B), and the common response to wheat stripe rust stress genes in the four time periods was 119.

Differential gene GO enrichment. The functions of the DEGs were divided into three categories in the GO enrichment analysis: biological processes, cellular components, and molecular functions (Figure 2, Table S3 in ESM). On the first day of inoculation with wheat stripe rust, AVS

Table 1. Summary statistics of clean data from the leaf tissue transcriptomes of two wheat varieties

Sample	ReadSum (Gb)	GC (%)	Error (%)	Q20 (%)	Q30 (%)
A1	9.71	53.51	0.026	97.56	93.70
A3	9.28	55.16	0.025	97.65	93.93
A5	9.21	53.50	0.026	97.45	93.48
A7	9.29	54.53	0.026	97.56	93.69
Y1	9.50	54.02	0.026	97.47	93.55
Y3	10.03	55.08	0.026	97.63	93.84
Y5	8.85	53.77	0.026	97.27	93.14
Y7	9.23	54.65	0.026	97.58	93.73

GC – guanine-cytosine

https://doi.org/10.17221/125/2022-PPS

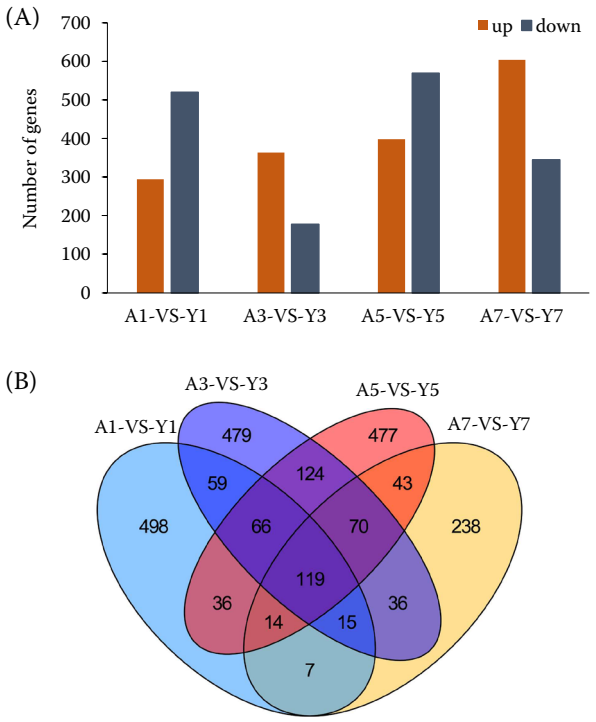

Figure 1. Statistical chart and Venn diagram of the differentially expressed genes (DEGs) at the four time points
(A) Statistical chart of the DEGs. DEGs were identified by filtering the two-fold up-regulated and down-regulated genes with false discovery rate ≤ 0.01. (B) Venn diagram of the DEGs. DEGs were identified by filtering the two-fold genes with false discovery rate ≤ 0.01

and AVSYr15NIL were compared, and the numbers of DEGs in biological processes and response to stress and defence were higher, involving 73 and 48 DEGs, respectively. Among the cell components, the numbers of genes in the periphery and plasma membrane were the largest, 79 and 73, respectively. Among molecular functions, 145 DEGs were involved in ion binding, and this was the most diverse group of genes in the GO classification. On the third day, biological regulation, intracellular and molecular function were the dominant categories. Defence response, cell periphery, and molecular function were the three dominant categories on the fifth day. The biosynthetic process, anchored component of membrane, and molecular function were the three highest categories on the seventh day.

Differentially expressed gene KEGG enrichment. The DEGs were analysed for KEGG enrichment, and on the first day of inoculation with wheat stripe rust, the results for AVS and AvsYr15NIL were compared. The main gene enrichment pathways were phenylpropanoid biosynthesis, the mitogen-activated protein kinase (MAPK) signalling pathway–plant, plant–pathogen interactions, and phenyl propionic acid biosynthesis. On the third day of inoculation with wheat stripe rust, the two groups of genes were enriched in carbon metabolism, the MAPK signalling pathway–plant and plant–pathogen interactions. On the fifth day of inoculation with wheat stripe rust, the two sets of genes were enriched in the biosynthesis of secondary metabolites, phenylpropanoid biosynthesis, and starch and sucrose metabolism; on day 7, the enriched metabolic pathways included plant-pathogen interactions, plant hormone signal transduction, and the MAPK signalling pathway–plant. The detailed information is listed in Table S4 in ESM.

Identification of candidate genes related to wheat stripe rust resistance. A total of 203 DEGs were screened from the KEGG pathway analysis. Nineteen DEGs involved in plant–pathogen interactions were identified, which involved several processes, including the response to stress, defence response, and response to biotic stimuli. DEGs were mapped to the MAPK signalling pathway–plant (19), plant hormone signal transduction (19), and phenyl propionic acid biosynthesis (12) in the KEGG database.

In the plant–pathogen interaction pathway for the response to stripe rust infection, the hypersensitive response, PAMP-triggered immunity (PTI), and effector-triggered immunity (ETI) were activated. PTI was activated via a calcium-dependent protein kinase (CDPK), calmodulin/calmodulin-like proteins (CaM/CMLs), respiratory burst oxidase homolog (Rboh), flagellin sensitive 2 (FLS2), and WRKY25/33. CDPK, CaM/CML, and Rboh belong to the Ca^{2+} pathway genes. The genes' resistance to *Pseudomonas syringae* pv. *maculicola* 1 (*RPM1*), *PTI1*, and heat shock protein 90 (*HSP90*) triggered *ETI* (Figure 3).

Validation of gene expression level by qRT-PCR. To identify and verify the genes associated with wheat stripe rust resistance, 12 DEGs that may be involved in stripe rust resistance were selected, including those associated with plant pathogen interactions, the MAPK signalling pathway, the Ras signaling pathway, and the Ca ion signalling pathway. The expression of transcriptional levels was verified using qRT-PCR. The qRT-PCR results for the DEGs were all consistent with the RNA-Seq

https://doi.org/10.17221/125/2022-PPS

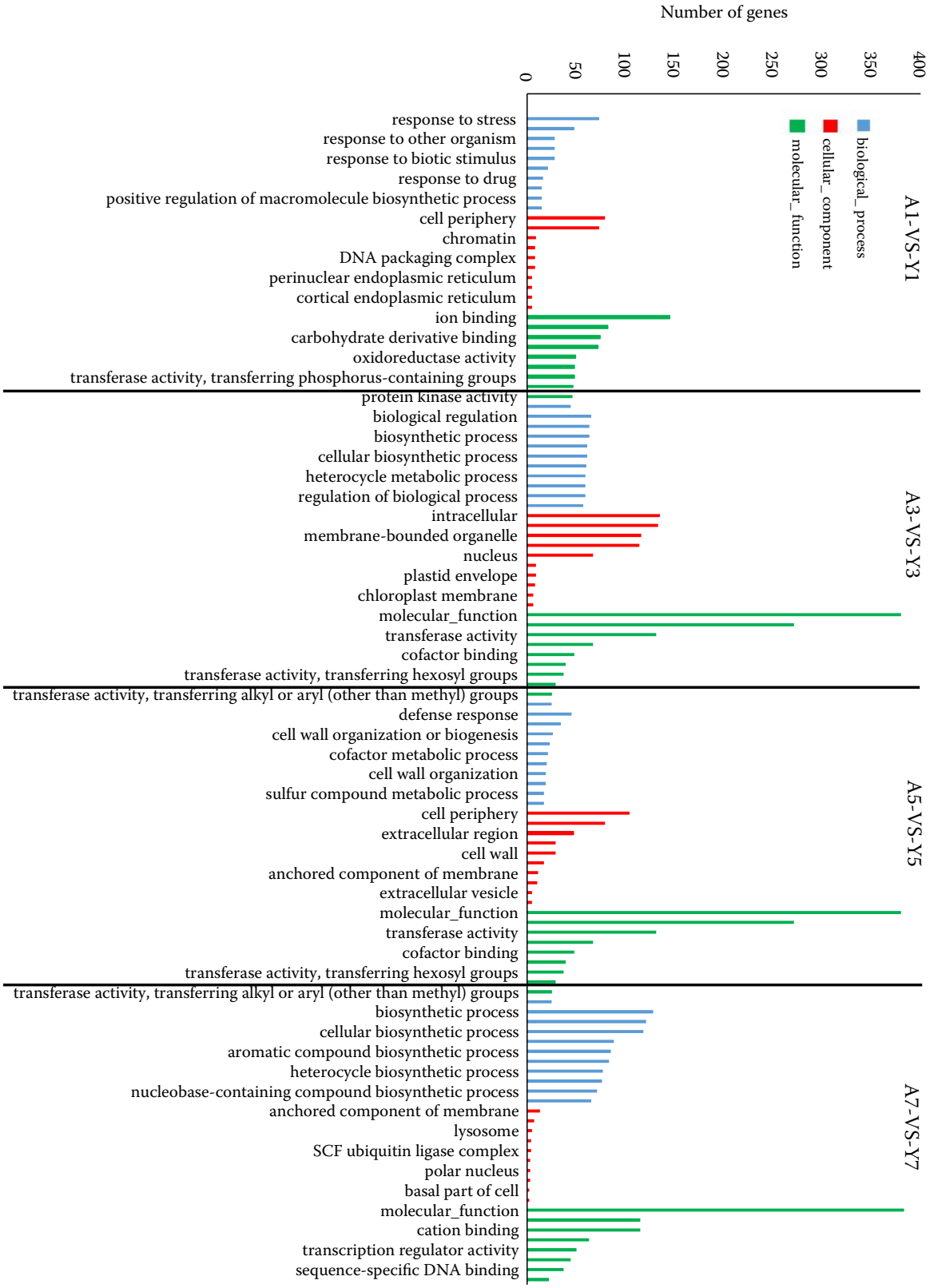

Figure 2. Gene Ontology annotation of the differentially expressed genes

Gene Ontology terms were identified by filtering with Q-value ≤ 0.05. The top 10 most significantly enriched biological processes (blue), cellular components (red), and molecular functions (green) were obtained from the A1-VS-Y1, A3-VS-Y3, A5-VS-Y5, and A7-VS-Y7

https://doi.org/10.17221/125/2022-PPS

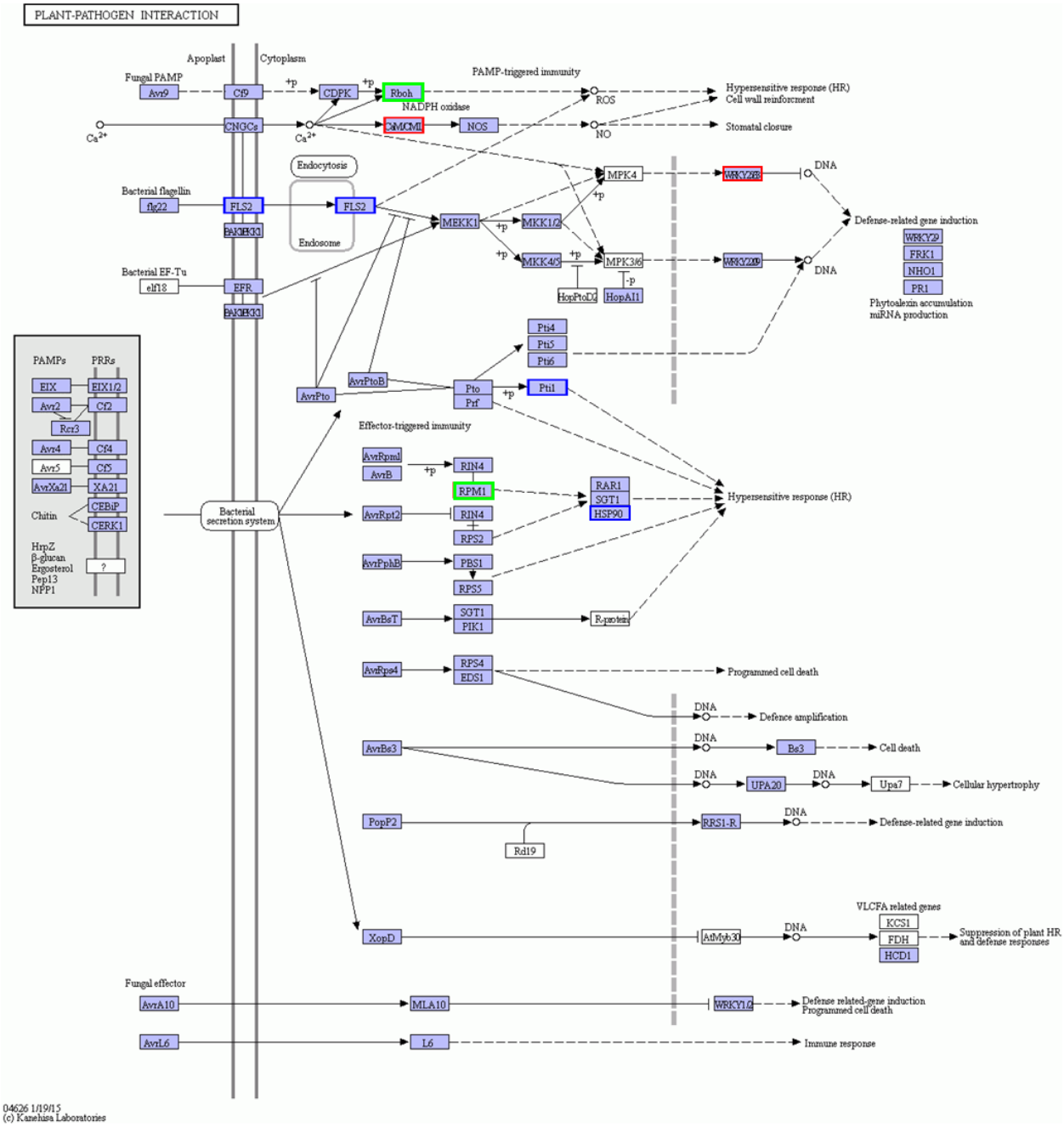

Figure 3. Annotated diagram of differentially expressed genes (DEGs) on the plant–pathogen interaction KEGG pathway

Red indicates that the DEGs encoding corresponding proteins were upregulated in comparison with mock-inoculation, blue indicates downregulation, and green indicates that the DEGs showed mixed expression

data, although the fold change had some inaccuracies. The relative expression levels of qRT-PCR for four DEGs were upregulated, namely TraesCS7B03G1204400.3 (HSP90B), TraesCS7D03G1221800 (HSP90B), TraesCS2B03G1346400 (tyrosine protein kinase) and TraesCS3D03G0735400 (UDP-glycosyltransferase-related gene). Eight DEGs with relative expression levels by qRT-PCR were down-regulated, namely TraesCS5B03G0981200 (RPS3), TraesCS3D03G0761900 (WRKY33), TraesCS3B03G1335600 (CML), TraesCS3D03G0074700 (CML), TraesCS5B03G0599000 (CALM), TraesCS6A03G0264300 (ubiquitinated family gene), TraesCS7A03G0146600 (GH3), and TraesCS7B03G0773900 (CML). The results suggested that the transcriptome data were reliable for analysis (Figure 4). These genes underwent

https://doi.org/10.17221/125/2022-PPS

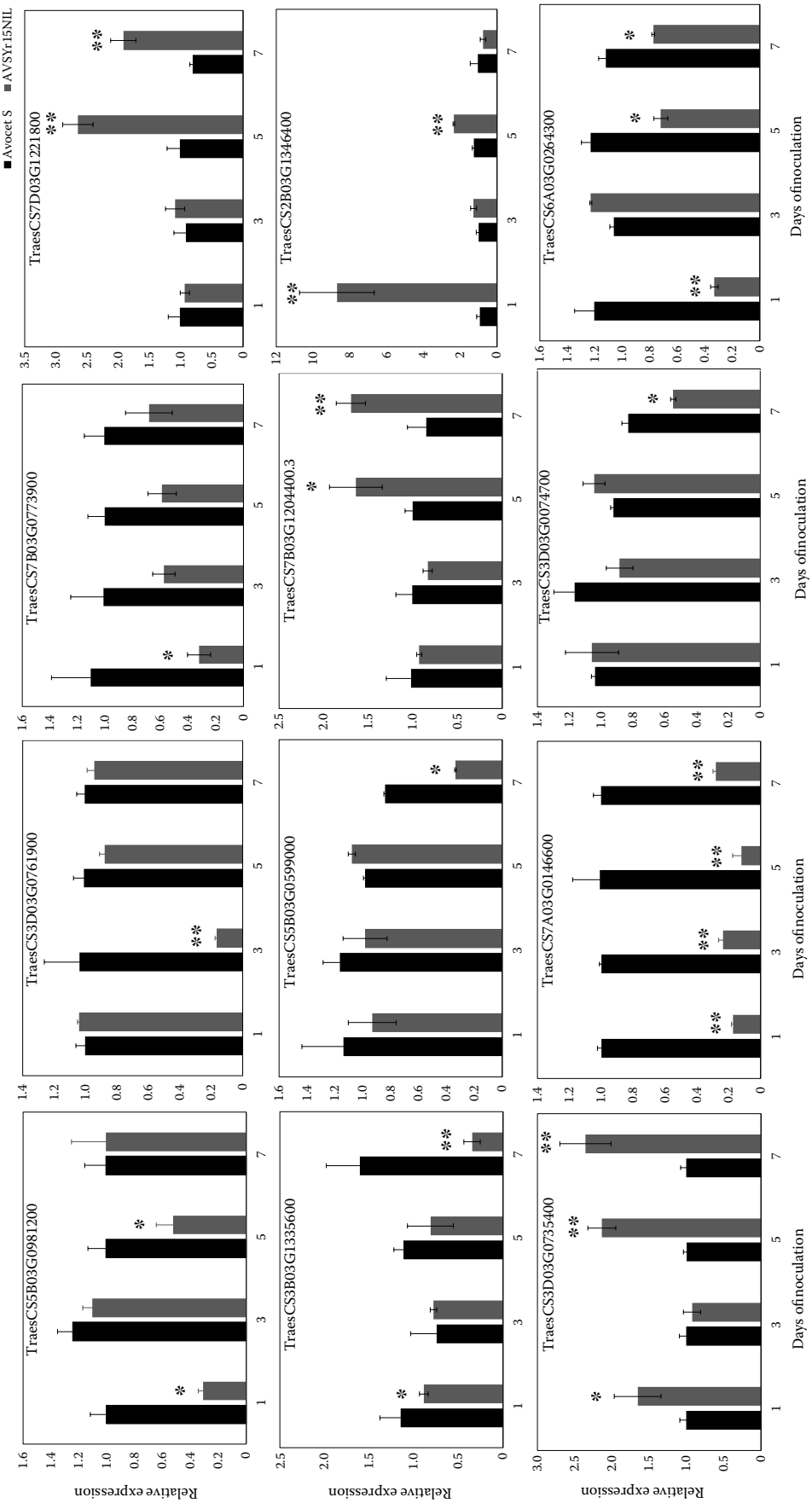

Figure 4. Quantitative real-time PCR analyses
Relative gene quantification was calculated using a comparative $2^{-\Delta\Delta CT}$ method. PR15 served as a control and mean ± SD of data from three biological replicates were plotted
*Value of two-way ANOVA $P < 0.05$; **value of two-way ANOVA $P < 0.01$

https://doi.org/10.17221/125/2022-PPS

expression changes induced by wheat stripe rust, indicating that they may be involved in the resistance to stripe rust.

DISCUSSION

Plant disease resistance is the result of mutual adaptation and selection between plants and their pathogens in long-term co-evolution. In the process of pathogen evolution, different forms and degrees of parasitism and pathogenicity affect host plants, and the plants accordingly develop different forms and degrees of disease resistance via a variety of genes and proteins (Andersen et al. 2018). In this study, transcriptomics technology was used to screen for differentially expressed genes after inoculation of CYR34 in the wheat susceptible stripe rust cultivar AVS and the AVS-dependent stripe rust-resistant near-genetic line AVSYr15NIL to identify mRNAs specific to the stripe rust response.

The results showed that the pathways of phenyl propionic acid biosynthesis, plant-pathogen interaction, and plant PPAR signalling were significantly enriched in the two cultivars at four time points. Most of the significantly differentially expressed genes contained in plant-pathogen interactions had EF-hand domains or protein kinase binding sites, and the basic modular structure of EF-hand proteins is helix-loop-helix, which enables this type of protein to recognise and transmit special calcium ion signals. Studies have shown that EF-hand calcitonin affects plant defence, aging, and response to environmental adversity. For example, the introduction of this gene from amoeba into tomatoes improved the tolerance of tomato plants to high salt stress (Pandey et al. 2002). In vegetative tissues, the EFA27 gene in rice (*Oryza sativa* L.). can be induced by exogenous abscisic acid and osmotic stress (Frandsen et al. 1996). In addition, the resistance to pathogenic bacteria conferred by this protein has also been reported, and calcium-binding protein products may be important factors leading to allergic necrosis pathways (Jakobek et al. 1999). The EF hand module encoded by the *EFA27* gene in rice is induced by abscisic acid and osmotic pressure in vegetative tissues (Zeng et al. 2017). Further screening of such genes finally selected four calmodulin (CML) genes containing EF-hand: TraesCS3B03G1335600, TraesCS3D03G0074700, TraesCS5B03G0599000, and TraesCS7B03G0773900. The proteins expressed by this type of gene bind calcium ions in plant cells. This process has an important function in the signal transduction of plant growth and development and stress. TaCAM2-D acts as a positive regulator in response to drought and is involved in salt tolerance in wheat (Li et al. 2022); the ShCML44 gene was used to improve abiotic stress tolerance in tomato (Munir et al. 2016). A large amount of evidence has demonstrated that CML plays an important role in the regulation of plant disease resistance. For example, in *Arabidopsis thaliana*, the gene *CML9* is induced by pathogenic bacteria, flagellin, and salicylic acid and plays a positive regulatory role in immune regulation (Leba et al. 2012). In plants, CaM/CML antagonists have been shown to affect pathogen-related nitric oxide (NO) generation and plant defence responses (Ma et al. 2008). The level of expression of the CML gene in beans was induced by pathogenic bacteria. Furthermore, the transcription level of CML gene in beans is related to initial symptoms of infection by non-pathogenic bacteria, and related to cell death caused by disease that is related to infection by pathogenic bacteria (Jakobek et al. 1999).

In addition, two heat shock protein genes were screened, TraesCS7B03G1204400 and TraesCS7D03G1221800. The transcriptome showed that both genes were present in the endoplasmic reticulum cavity, and a literature search showed that such proteins often participate in various metabolic pathways in the form of chaperones in the process of plant growth. In addition, these proteins play important roles in the growth and development process as well as in metabolic regulation and biotic and abiotic stress responses of plants. For example, the *Hsp26* gene is involved in seed maturation and germination and imparts tolerance to heat stress (Chauhan et al. 2012), and heat-shock proteins are involved in the powdery mildew and stripe rust resistance mechanisms of wheat (Guo et al. 2021). Twelve DEGs that may be involved in stripe rust resistance have been verified, and the trends are consistent with those shown by transcriptome data. Interestingly, TraesCS2B03G1346400, which belong to tyrosine protein kinase gene family, was found by qRT-PCR, and its expression was significantly increased in AVSYr15NIL on the first day after inoculation. Most research on this gene has focused on animals, and the results have shown that it plays an important role in several forms

https://doi.org/10.17221/125/2022-PPS

of cancer (Sun & Ayrapetov 2023); however, little research on this gene has been carried out in plants. This gene may be key to disease resistance, and its specific function requires further study.

This study provides a theoretical and practical basis for the cultivation of wheat varieties with broad-spectrum, stable, and durable disease resistance.

CONCLUSION

In this study, we performed transcriptome analyses of the stripe rust susceptible cultivar AVS and AVS-dependent stripe rust-resistant near-genetic line AVSYr15NIL. Seedlings were inoculated with CYR34 and sampled at four time points. Candidate genes related to stripe rust resistance were identified and involved in defence response, response to stress, biological regulation, regulation of response to stimulus, and response to a biotic stimulus. KEGG analysis showed that the DEGs were most enriched in plant–pathogen interactions, phenylpropanoid biosynthesis, the MAPK signalling pathway–plant, and plant hormone signal transduction. Further functional analysis of important candidate genes related to stripe rust provided crucial clues regarding the mechanisms underlying stripe rust resistance in wheat.

REFERENCES

Andersen E.J., Ali S., Byamukama E., Yen Y., Nepal M.P. (2018): Disease resistance mechanisms in plants. Genes, 9: 339. doi: 10.3390/genes9070339

Cantu D., Pearce S.P., Distelfeld A., Christiansen M.W., Uauy C., Akhunov E., Fahima T., Dubcovsky J. (2011): Effect of the down-regulation of the high grain protein content (GPC) genes on the wheat transcriptome during monocarpic senescence. BMC Genomics, 12: 1–17.

Chauhan H., Khurana N., Nijhavan A., Khurana J.P., Khurana P. (2012): The wheat chloroplastic small heat shock protein (sHSP26) is involved in seed maturation and germination and imparts tolerance to heat stress. Plant Cell and Environment, 35: 1912–31.

Chen X.M. (2005): Epidemiology and control of stripe rust (*Puccinia striiformis* f. sp. *tritici*) on wheat. Canadian Journal of Plant Pathology, 27: 314–37.

Chen X.M. (2013): High-temperature adult-plant resistance, key for sustainable control of stripe rust. American Journal of Plant Sciences, 4: 608–27.

Chen X.M. (2014): Integration of cultivar resistance and fungicide application for control of wheat stripe rust. Canadian Journal of Plant Pathology, 36: 311–26.

Colgan A.M., Cameron A.D., Kröger C. (2017): If it transcribes, we can sequence it: Mining the complexities of host-pathogen-environment interactions using RNA-seq. Current Opinion in Microbiology, 36: 37–46.

Corredor-Moreno P., Minter F., Davey P.E., Wegel E., Kular B., Brett P., Lewis C.M., Morgan Y.M.L., Macías Pérez L.A., Korolev A.V., Hill L., Saunders D.G.O. (2021): The branched-chain amino acid aminotransferase TaBCAT1 modulates amino acid metabolism and positively regulates wheat rust susceptibility. The Plant Cell, 33: 1728–47.

Duan X.Y., Wang X.J., Fu Y.P., Tang C.L., Li X.R., Cheng Y.L., Hao F., Huang L.L., Kang Z. (2013): TaEIL1, a wheat homologue of AtEIN3, acts as a negative regulator in the wheat–stripe rust fungus interaction. Molecular Plant Pathology, 14: 728–39.

Ebeed H.T. (2022): Genome-wide analysis of polyamine biosynthesis genes in wheat reveals gene expression specificity and involvement of STRE and MYB-elements in regulating polyamines under drought. BMC Genomics, 23: 734. doi: 10.1186/s12864-022-08946-2

Frandsen G., Müller-Uri F., Nielsen M., Mundy J., Skriver K. (1996): Novel plant Ca^{2+}-binding protein expressed in response to abscisic acid and osmotic stress. Journal of Biology Chemistry, 271: 343–8.

Guo H., Zhang H., Wang G.H., Wang C.Y., Wang Y.J., Liu X.L., Ji W.Q. (2021): Identification and expression analysis of heat-shock proteins in wheat infected with powdery mildew and stripe rust. Plant Genome, 14: e20092. doi: 10.1002/tpg2.20092

Haider M.S., Zhang C., Kurjogi M.M., Pervaiz T., Zheng T., Zhang C.B., Chen L.D., Shangguan L.F., Fang J.G. (2017): Insights into grapevine defense response against drought as revealed by biochemical, physiological and RNA-Seq analysis. Scientific Reports, 7: 1–15.

Jakobek J.L., Smith-Becker J.A., Lindgren P.B. (1999): A bean cDNA expressed during a hypersensitive reaction encodes a putative calcium-binding protein. Molecular Plant-Microbe Interactions, 12: 712–9.

Klymiuk V., Yaniv E., Huang L., Raats D., Fatiukha A., Chen S.S., Feng L.H., Frenkel Z., Krugman T., Lidzbarsky G., Chang W., Jääskeläinen M.J., Schudoma C., Paulin L., Laine P., Bariana H., Sela H., Saleem K., Sørensen C.K., Hovmøller M.S., Distelfeld A., Chalhoub B., Dubcovsky J., Korol A.B., Schulman A.H., Fahima T. (2018): Cloning of the wheat *Yr15* resistance gene sheds light on the plant tandem kinase-pseudokinase family. Nature Communications, 9: 3735. doi: 10.1038/s41467-018-06138-9

https://doi.org/10.17221/125/2022-PPS

Leba L.J., Cheval C., Ortiz-Martín I., Ranty B., Beuzón C.R., Galaud J.P., Aldon D. (2012): CML9, an Arabidopsis calmodulin-like protein, contributes to plant innate immunity through a flagellin-dependent signalling pathway. Plant Journal, 71: 976–89.

Lee M.H., Kim K.M., Sang W.G., Kang C.S., Choi C. (2022): Comparison of gene expression changes in three wheat varieties with different susceptibilities to heat stress using RNA-seq analysis. International Journal of Molecular Sciences, 23: 10734. doi: 10.3390/ijms231810734

Li Y.Q., Zhang H.D., Dong F.Y., Zou J., Gao C.B., Zhu Z.W., Liu Y.K. (2022): Multiple roles of wheat calmodulin genes during stress treatment and TaCAM2-D as a positive regulator in response to drought and salt tolerance. International Journal of Biological Macromolecules, 220: 985–97.

Ma W., Smigel A., Tsai Y.C., Braam J., Berkowitz G.A. (2008): Innate immunity signaling: Cytosolic Ca^{2+} elevation is linked to downstream nitric oxide generation through the action of calmodulin or a calmodulin-like protein. Plant Physiology, 148: 818–28.

Ma P.T., Wu L.R., Xu Y.F., Xu H.X., Zhang X., Wang W.R., Liu C., Wang B. (2021): Bulked segregant RNA-seq provides distinctive expression profile against powdery mildew in the wheat genotype YD588. Frontiers in Plant Science, 12: 764978. doi: 10.3389/fpls.2021.764978

Munir S., Liu H., Xing Y.L., Hussain S., Ouyang B., Zhang Y.Y., Li H.X., Ye Z.B. (2016): Overexpression of calmodulin-like (ShCML44) stress-responsive gene from *Solanum habrochaites* enhances tolerance to multiple abiotic stresses. Scientific Reports, 6: 1–20.

Pandey G.K., Reddy V.S., Reddy M.K., Deswal R., Bhattacharya A., Sopory S.K. (2002): Transgenic tobacco expressing *Entamoeba histolytica* calcium binding protein exhibits enhanced growth and tolerance to salt stress. Plant Science, 162: 41–7.

Sun G.Q., Ayrapetov M.K. (2023): Dissection of the catalytic and regulatory structure-function relationships of Csk protein tyrosine kinase. Frontiers in Cell and Developmental Biology, 11: 1148352. doi: 10.3389/fcell.2023.1148352

Qie Y.M., Liu Y., Wang M.N., Li X., See D.R., An D.G., Chen X.M. (2019): Development, validation, and re-selection of wheat lines with pyramided genes *Yr64* and *Yr15* linked on the short arm of chromosome 1B for resistance to stripe rust. Plant Disease, 103: 51–8.

Vranic M., Perochon A., Benbow H., Doohan F.M. (2022): Comprehensive analysis of pathogen-responsive wheat NAC transcription factors: new candidates for crop improvement. G3, 12: jkac247. doi: 10.1093/g3journal/jkac247

Wan A.M., Chen X.M. (2012): Virulence, frequency, and distribution of races of *Puccinia striiformis* f. sp. *tritici* and *P. striiformis* f. sp. *hordei* identified in the United States in 2008 and 2009. Plant Disease, 96: 67–74.

Wang B., Wei J.P., Song N., Wang N., Zhao J., Kang Z.S. (2018): A novel wheat NAC transcription factor, TaNAC30, negatively regulates resistance of wheat to stripe rust. Journal of Integrative Plant Biology, 60: 432–43.

Wang Y.Q., Liu C., Du Y.Y., Cai K.Y., Wang Y.F., Guo J., Guo J., Bai X.X., Kang Z.S., Guo J. (2022): A stripe rust fungal effector PstSIE1 targets TaSGT1 to facilitate pathogen infection. Plant Journal, 112: 1413–28.

Wellings C.R. (2011): Global status of stripe rust: A review of historical and current threats. Euphytica, 179: 129–41.

Xu L., Zhu L.F., Tu L.L., Liu L.L., Yuan D.J., Jin L., Lu L., Zhang X.L. (2011): Lignin metabolism has a central role in the resistance of cotton to the wilt fungus *Verticillium dahliae* as revealed by RNA-Seq-dependent transcriptional analysis and histochemistry. Journal of Experimental Botany, 62: 5607–21.

Zeng H.Q., Zhang Y.X., Zhang X.J., Pi E.X., Zhu Y.Y. (2017): Analysis of EF-hand proteins in soybean genome suggests their potential roles in environmental and nutritional stress signaling. Frontiers in Plant Science, 8: 877. doi: 10.3389/fpls.2017.00877

Zhang X.B., Ma Q., Li F.J., Ding Y.G., Yi Y., Zhu M., Ding J.F., Li C.Y., Guo W.S., Zhu X.K. (2021): Transcriptome analysis reveals different responsive patterns to nitrogen deficiency in two wheat near-isogenic lines contrasting for nitrogen use efficiency. Biology, 10: 1126. doi: 10.3390/biology10111126

Zhao J., Wang M.N., Chen X.M., Kang Z.S. (2016): Role of alternate hosts in epidemiology and pathogen variation of cereal rusts. Annual Review of Phytopathology, 54: 207–28.

Zhao F.Y., Niu K.J., Tian X.H., Du W.H. (2022): Triticale improvement: Mining of genes related to yellow rust resistance in triticale based on transcriptome sequencing. Frontiers in Plant Science, 13: 883147. doi: 10.3389/fpls.2022.883147

Received: November 19, 2022
Accepted: April 28, 2023
Published online: May 17, 2023